

## Search for SM Higgs Decaying to ZZ to $\ell^- \ell^+ q \bar{q}$ or $\ell^- \ell^+ \nu \bar{\nu}$ at CMS

---

**Francesco Pandolfi\***

On behalf of the CMS Collaboration

ETH Zurich IPP

E-mail: [francesco.pandolfi@cern.ch](mailto:francesco.pandolfi@cern.ch)

A report on two searches for the Standard Model Higgs boson, performed respectively in the  $H \rightarrow ZZ \rightarrow \ell^- \ell^+ q \bar{q}$  and  $H \rightarrow ZZ \rightarrow \ell^- \ell^+ \nu \bar{\nu}$  decay channels, is presented. The  $H \rightarrow ZZ \rightarrow \ell^- \ell^+ q \bar{q}$  search analyzes  $4.6 \text{ fb}^{-1}$  of 7 TeV collision data. No significant excess with respect to the background hypothesis is observed, therefore upper limits on the Higgs boson production cross section are set in the range of masses between 130 GeV and 600 GeV, reaching sensitivity to the Standard Model production in the 370 – 400 GeV interval. The  $H \rightarrow ZZ \rightarrow \ell^- \ell^+ \nu \bar{\nu}$  analysis is extended also to  $5 \text{ fb}^{-1}$  of 8 TeV data and can exclude Standard Model production of a Higgs boson at the 95% CL in the mass range of 278-600 GeV.

*36th International Conference on High Energy Physics*

*4-11 July 2012*

*Melbourne, Australia*

---

\*Speaker.

## 1. Introduction

The search for Standard Model Higgs boson has always been a combined effort. As its mass ( $m_H$ ) is a free parameter of the theoretical model, the full allowed mass range (between the LEP limit of 115 GeV and the energetic boundary of  $\approx 600$  GeV, after which Higgs couplings are not finite) had to be explored by the experiments. Probing such a vast energy range means exploiting different Higgs decay channels, as the possibilities change with the increasing mass.

For Higgs masses heavy enough to energetically allow the decay to pairs of electroweak vector bosons, these decay channels are the ones dominating the search strategies. Among the decays to  $Z$  boson pairs, three decay chains drive the effort: the ‘golden’ fully leptonic final state ( $H \rightarrow ZZ \rightarrow 4\ell$ ), the leptonic final state with neutrinos ( $H \rightarrow ZZ \rightarrow \ell^- \ell^+ \nu\bar{\nu}$ ) and the semileptonic one ( $H \rightarrow ZZ \rightarrow \ell^- \ell^+ q\bar{q}$ ), where everywhere in this article we use the letter  $\ell$  to denote electrons or muons. Compared to the golden leptonic decay channel, the two latter final states benefit from more favorable branching ratios, so that their effective cross section is, respectively, about 6 and 20 times larger than the golden channel. On the other hand, the intrinsic complexity of jet and missing transverse energy reconstruction, as well as the higher level of expected backgrounds, pose more demanding experimental challenges to these analyses.

This report presents the results of the search for a Standard Model Higgs boson in the  $H \rightarrow ZZ \rightarrow \ell^- \ell^+ q\bar{q}$  [1] and  $H \rightarrow ZZ \rightarrow \ell^- \ell^+ \nu\bar{\nu}$  [2, 3] decay channels. The results are based on proton-proton collision data recorded in 2011 and 2012 by the CMS experiment at the CERN LHC. The results from the search performed in the  $H \rightarrow ZZ \rightarrow \ell^- \ell^+ q\bar{q}$  channel are based on  $4.6 \text{ fb}^{-1}$  of data collected at a center of mass energy  $\sqrt{s} = 7 \text{ TeV}$  in 2011, whereas the  $H \rightarrow ZZ \rightarrow \ell^- \ell^+ \nu\bar{\nu}$  analysis also includes  $5 \text{ fb}^{-1}$  recorded at  $\sqrt{s} = 8 \text{ TeV}$  in 2012.

## 2. The $H \rightarrow ZZ \rightarrow \ell^- \ell^+ q\bar{q}$ Analysis

The  $H \rightarrow ZZ \rightarrow \ell^- \ell^+ q\bar{q}$  channel is conceptually similar to the  $H \rightarrow ZZ \rightarrow 4\ell$  channel: the four-momenta of the four final state decay products are completely reconstructed in the detector. The search is therefore performed as a search for an invariant mass peak over a background spectrum. The main differences between the two channels is the presence of jets in the final state, which can significantly deteriorate the Higgs mass resolution and increase the level of backgrounds.

In order to minimize the effect of jet energy resolution on the reconstructed invariant mass of the signal which is searched for, a kinematic fit is enforced on the dijet system. This fit constrains the dijet invariant mass to the nominal  $Z$  boson mass, and does so by fully taking into account the jet energy and angular resolutions as a function of the jet pseudorapidity and transverse momentum, leading to a significant improvement in the expected  $m_H$  resolution.

A cardinal point of this analysis is understanding that jet flavor may provide a powerful means of background discrimination. Jets in signal events are produced in hadronic decays of a  $Z$  boson, and therefore originate from the hadronization of quark partons. The flavor of quarks in  $Z$  decays is almost equally distributed among the five types  $d$ ,  $u$ ,  $s$ ,  $c$ ,  $b$ . The dominant background is represented by a leptonically-decaying  $Z$  boson produced in association with hard jets, a process in which gluon radiation is expected to play a major role. In addition to gluons,  $u$  and  $d$  quarks, valence partons of the protons, dominate the jet production associated with the  $Z$ .

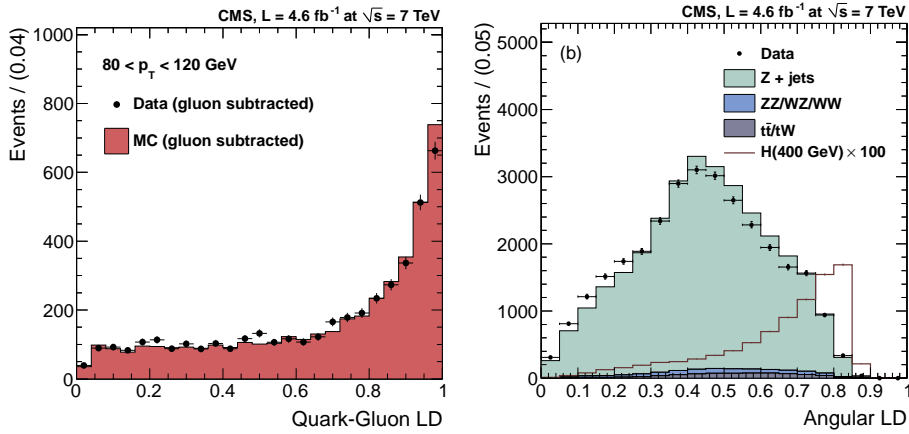


**Figure 1:** Left: distribution of the quark-gluon LD in  $\gamma$ +jet events, for jets with transverse momenta between 80 and 120 GeV. Right: distribution of the angular LD in data and in the main backgrounds after loose event selections. A hypothetical signal with a mass of 400 GeV and cross section 100 times that of the Higgs boson is superimposed.

Two directives have therefore been pursued:

- the isolation of events with jets which are compatible with the hadronization of  $b$  quarks, aiming to isolate the  $Z \rightarrow b\bar{b}$  contribution, which is only a fraction of the total signal but is faced with drastically lower levels of backgrounds;
- the identification and rejection of jets compatible with gluon hadronization.

The first directive has led to the categorization in three exclusive categories, depending on the amount of jets (either 0, 1 or  $\geq 2$ ) in the final state which have been found compatible with the hadronization of a bottom quark ( $b$ -tags). The second to the use of a likelihood discriminant (LD) which, by studying the particle composition of the reconstructed jets, is able to distinguish between light quark and gluon hadronization. Figure 1 (left) shows the distribution, in data and in the Monte Carlo simulation, of the quark-gluon LD for jets in  $\gamma$ +jet events (which are dominated by light quark jets) with transverse momentum between 80 and 120 GeV. As can be seen, the discriminant peaks at one, as is expected for quark jets, and no significant discrepancy between data and the simulation is observed.

The kinematic discrimination between signal and background is performed through an angular analysis, based on the study presented in [4]. Five angles univocally determine the final state of the decay chain. These angles are reconstructed from the four-momenta of the reconstructed objects of the final state and are used to build a five-dimensional likelihood discriminant capable of selecting events compatible with the hypothesis that the four objects come from the signal decay chain. The use of an angular approach has also the advantage of preserving the background shape, simplifying the background estimation procedure. The distribution of the angular discriminant, in data and simulation events passing loose event selection requirements, is shown in Figure 1 (right). The data points are compared to the different contributions of the simulated backgrounds, and the expected distribution for events arising from the decay of a Higgs boson with  $m_H = 400$  GeV is superimposed, scaled by a factor 100.

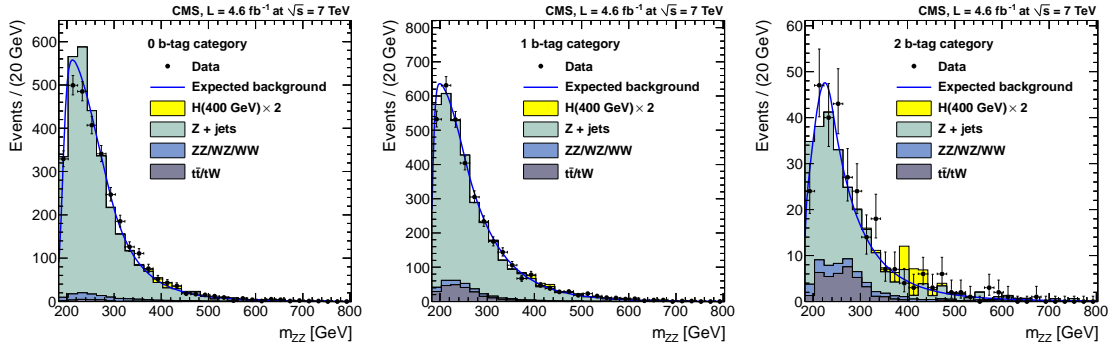


**Figure 2:** The invariant mass distribution after final selection in three categories: 0  $b$ -tag (left), 1  $b$ -tag (middle), and 2  $b$ -tag (right). Points with error bars show distributions of data and solid curved lines show the prediction of background. For illustration solid histograms depict the background expectation from simulated events with the different components illustrated. Also shown is a hypothetical signal with a mass of 400 GeV and cross section two times that of the Higgs boson.

After the full set of event selection requirements is enforced, the invariant mass spectra shown in Figure 2 are obtained, respectively in the three  $b$ -tag categories. The data points can be compared to the blue lines, which represent the background expectation in each category as obtained from control regions and superimposed to the signal regions. The good agreement between the data points and the background estimations indicate that the latter are robust, and the absence of marked excesses allows us to impose an upper limit on Standard Model Higgs production.

The analysis has been extended to the low mass region ( $125 < m_H < 170$  GeV), searching for the decay  $H \rightarrow Z^* Z \rightarrow \ell^- \ell^+ q\bar{q}$ , in which the virtual  $Z$  boson is requested to decay to leptons. The analysis is conceptually similar to the high mass search, but the angular and quark-gluon likelihood discriminants have been dropped.

The resulting invariant mass spectra obtained in the three categories of the high (low) mass analysis are statistically analyzed in the 183 – 600 (130 – 164) GeV ranges and interpreted as 95% confidence level upper limits on the Higgs production cross section for the relative masses. The limits are computed with the  $CL_s$  [5] method and are shown in Figure 3. As can be seen, no evidence for Higgs boson production is observed. The low mass analysis excludes a cross section three times the Standard Model around 155 GeV, whereas the high mass analysis reaches sensitivity to the Standard Model expectation in the 370 – 400 GeV interval.

### 3. The $H \rightarrow ZZ \rightarrow \ell^- \ell^+ \nu\bar{\nu}$ Analysis

In the  $H \rightarrow ZZ \rightarrow \ell^- \ell^+ \nu\bar{\nu}$  analysis, one of the two  $Z$  bosons is required to decay to neutrinos. These particles are not reconstructed in the detector, therefore the kinematics of the final state are not fully known. Rather, the presence of the invisible  $Z$  decay will manifest as missing transverse energy ( $E_T^{\text{miss}}$ ). In order to effectively contrast background processes in which the  $E_T^{\text{miss}}$  arises from instrumental sources, such as resolution effects, only events in which a significant amount of  $E_T^{\text{miss}}$  is produced are sought for. This translates into the requirement that the decaying Higgs boson has a mass significantly higher than that of its decays products ( $m_H \geq 200$  GeV), so that the latter will have a strong Lorentzian boost in the laboratory frame.

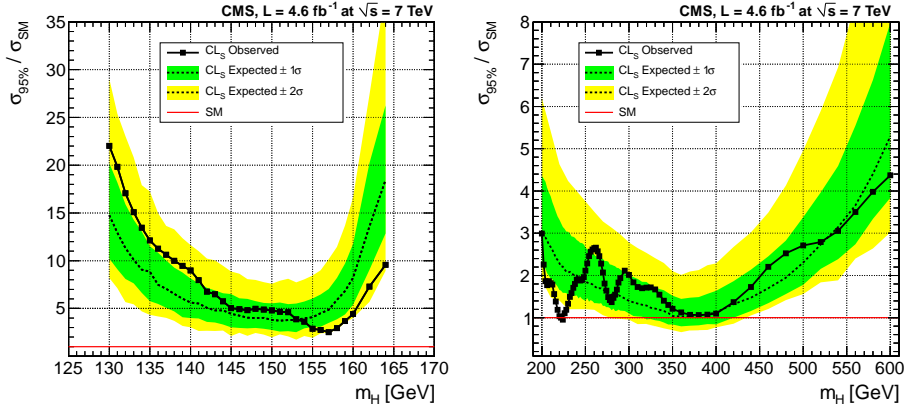


**Figure 3:** Observed (solid) and expected (dashed) 95% CL upper limit on the ratio of the production cross section to the SM expectation for the Higgs boson obtained using the  $CL_s$  technique in the  $H \rightarrow ZZ \rightarrow \ell^-\ell^+q\bar{q}$  analysis. The 68% and 95% ranges of expectation for the background-only model are also shown with green and yellow bands, respectively. The solid line at 1 indicates the SM expectation. Left: low mass range, right: high mass range.

At the end of 2011, most of the allowed values of  $m_H$  in the high mass range have been excluded by the results of the direct searches performed at LHC. Nevertheless, the nature of longitudinally polarized  $W$  boson scattering at high invariant masses still must be understood. This is why, in recent developments of this analysis, special attention was given to events compatible with the electroweak vector boson (VBF) signal production mechanism.

Two broad analysis categories are therefore defined:

- **VBF category:** events which present two jets in the forward region with pseudorapidity gap  $|\Delta\eta| > 4$  and minimal invariant mass of 500 GeV. The two leptons forming the  $Z$  candidate are requested to lie between these two jets, while no other selected jets are allowed in this central region;
- **Gluon fusion category:** all events failing the VBF selection are divided according to the number of reconstructed jets with  $p_T > 30$  GeV into three additional categories ( $N_{\text{jets}} = 0, 1,$  and  $\geq 2$ ).

The kinematical selection is based on three variables: the missing transverse energy of the event  $E_T^{\text{miss}}$ , the transverse momentum of the reconstructed  $Z$  boson  $p_{T,Z}$  and the transverse mass  $M_T$ , defined by:

$$M_T^2 = \left( \sqrt{p_{T,Z}^2 + M_Z^2} + \sqrt{E_T^{\text{miss}2} + M_Z^2} \right)^2 - \left( \vec{p}_{T,Z} + \vec{E}_T^{\text{miss}} \right)^2,$$

where  $M_Z$  indicates the dilepton invariant mass. In the VBF category, mass-independent requirements are enforced in the form  $p_{T,Z} > 55$  GeV and  $E_T^{\text{miss}} > 70$  GeV, whereas in the three gluon fusion categories optimized, mass-dependent selections on  $E_T^{\text{miss}}$  and  $M_T$  are applied.

The reconstructed  $E_T^{\text{miss}}$  represents the main tool of background discrimination. The dominant background process is constituted by Drell-Yan ( $Z \rightarrow \ell\ell$ )+ $E_T^{\text{miss}}$  events, in which the reconstructed missing transverse energy is originated by instrumental and reconstruction effects. It has been

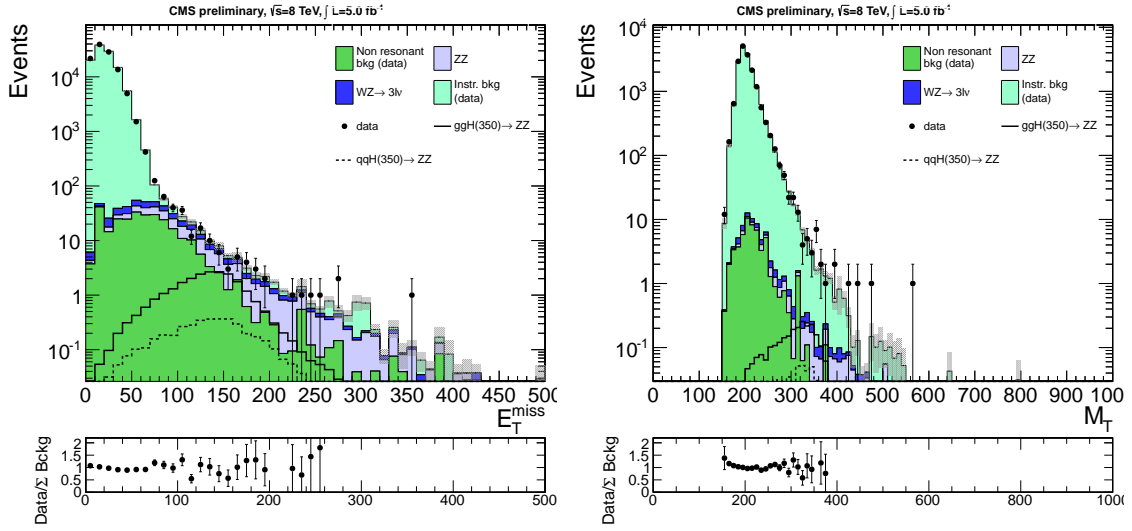


**Figure 4:** Comparisons of the  $E_T^{\text{miss}}$  (left) and  $M_T$  (right) distributions in  $5 \text{ fb}^{-1}$  of 8 TeV data to the background expectations, after loose event selection requirements. Superimposed are also shown the expected distributions for a 350 GeV signal, both for the gluon fusion (solid) and VBF (dashed) production processes.

chosen not to rely on the Monte Carlo simulation for the description of such non-physical  $E_T^{\text{miss}}$ . Instead, a control sample in the data has been identified in  $\gamma+E_T^{\text{miss}}$  events. Because of the excellent resolution of the CMS electromagnetic calorimeter, photons are reconstructed with very high accuracy, similarly to a  $Z$  boson decaying to electron or muon pairs. These two classes of events, therefore, will have similar distributions of instrumental  $E_T^{\text{miss}}$ , with the advantage that the larger  $\gamma$ +jet cross section allows for greater statistical power. In order for  $\gamma+E_T^{\text{miss}}$  events to have the same kinematic properties of  $Z+E_T^{\text{miss}}$  events, a reweighting procedure is applied, based on the transverse momentum of the boson and the reconstructed vertex multiplicity.

Other notable background processes to this channel are non-resonant dilepton events ( $t\bar{t}$ ,  $WW$ ) and resonant dilepton events arising from continuous diboson production ( $ZZ$ ,  $WZ$ ). The latter are taken from the Monte Carlo simulation. Non-resonant events are symmetric in same-flavor ( $ee$ ,  $\mu\mu$ ) and cross-flavor ( $e\mu$ ) combinations, so cross-flavor events can be used to normalize the expected yield for these processes. This is done through a sideband ratio procedure: the dilepton invariant mass is used to define, next to the signal region  $70 < M_Z < 110 \text{ GeV}$ , two sideband regions:  $50 < M_Z < 70 \text{ GeV}$  and  $110 < M_Z < 200 \text{ GeV}$ . The expected same-flavor signal region yield  $N_{\ell\ell}$  is then computed from the ratio of the sideband yields  $N_{\ell\ell}^{\text{SB}}$  and the cross-flavor signal yield  $N_{e\mu}^{\text{sig}}$ :

$$N_{\ell\ell}^{\text{sig}} = \left( \frac{N_{\ell\ell}^{\text{SB}}}{N_{e\mu}^{\text{SB}}} \right) \cdot N_{e\mu}^{\text{sig}}.$$

Figure 4 compares the distributions of  $E_T^{\text{miss}}$  (left) and  $M_T$  (right) in  $5 \text{ fb}^{-1}$  of 8 TeV data to the background expectations, after loose event selection requirements. As can be seen, the good agreement between the data and the background estimations build confidence that the latter are robust, both in the bulk of the distributions, dominated by Drell-Yan events, and in the  $E_T^{\text{miss}}$  tail, in which the other background processes play a major role. Superimposed are also shown

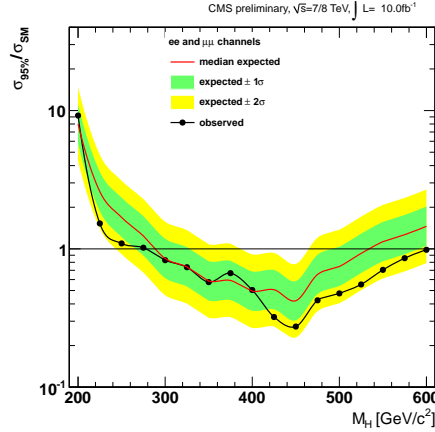


**Figure 5:** Observed (black) and expected (red) 95% CL upper limit on the ratio of the production cross section to the SM expectation for the Higgs boson obtained using the  $CL_s$  technique in the  $H \rightarrow ZZ \rightarrow \ell^-\ell^+\nu\bar{\nu}$  analysis. The 68% and 95% ranges of expectation for the background-only model are also shown with green and yellow bands, respectively. The solid line at 1 indicates the SM expectation.

the expected distributions for a 350 GeV signal, both for gluon fusion (solid) and VBF (dashed) production processes.

After the full set of event selection requirements is applied, the observed yields in data are compared to the background and signal expectations for different  $m_H$  hypotheses in the 200 – 600 GeV range, and interpreted as upper limits on the Higgs production cross section with the  $CL_s$  technique. The results are shown in Figure 5. No evidence for a Standard Model Higgs is reported, and this channel alone is capable of excluding its presence in the  $278 < m_H < 600$  GeV range with 95% confidence level.

#### 4. Conclusions

We have reported on two searches for the Standard Model Higgs boson, performed respectively in the  $H \rightarrow ZZ \rightarrow \ell^-\ell^+q\bar{q}$  and  $H \rightarrow ZZ \rightarrow \ell^-\ell^+\nu\bar{\nu}$  decay channels. The  $H \rightarrow ZZ \rightarrow \ell^-\ell^+q\bar{q}$  search analyzes  $4.6 \text{ fb}^{-1}$  of 7 TeV collision data. It is pursued in three  $b$ -tag categories, makes use of a kinematic fit to mitigate the effect of finite jet energy resolution, of an angular likelihood to discriminate events compatible with the decay of a Higgs boson from non-resonant backgrounds, and a quark-gluon likelihood discriminant. It sets limits in the 130 – 164 and 183 – 600 GeV mass ranges, reaching sensitivity to the Standard Model cross section in the 370 – 400 GeV interval.

The  $H \rightarrow ZZ \rightarrow \ell^-\ell^+\nu\bar{\nu}$  analysis is extended also to  $5 \text{ fb}^{-1}$  of 8 TeV data, and is performed in two broad categories, one specialized in the identification of VBF signal production, and one for gluon fusion production, the latter further subdivided in three jet multiplicity categories. It makes use of a completely data-driven approach to estimate the background arising by instrumental missing transverse energy in  $(Z \rightarrow \ell\ell) + E_T^{\text{miss}}$  events, based on  $\gamma + E_T^{\text{miss}}$  events. This analysis alone can exclude Standard Model production of a Higgs boson at the 95% CL in the mass range of 278-600 GeV.

## References

- [1] CMS Collaboration, *Search for a Higgs boson in the decay channel  $H \rightarrow ZZ^* \rightarrow q\bar{q}\ell^- \ell^+$  in pp collisions at  $\sqrt{s} = 7$  TeV*, *JHEP* **1204** (2012) 036 [[arXiv:1202.1416](#)].
- [2] CMS Collaboration, *Search for the standard model Higgs boson in the  $H \rightarrow ZZ \rightarrow 2\ell 2\nu$  channel in pp collisions at  $\sqrt{s} = 7$  TeV*, *JHEP* **1202** (2012) 040 [[arXiv:1202.3478](#)].
- [3] CMS Collaboration, *Higgs to ZZ to 2l 2nu*, CMS-PAS-HIG-12-023, 2012.
- [4] Y. Gao, A.V. Gritsan, Z. Guo, K. Melnikov, M. Schulze, and N.V. Tran, *Spin determination of single-produced resonances at hadron colliders*, *Phys. Rev. D*, 81:075022, 2010 [[arXiv:1001.3396](#)].
- [5] A.L. Read, *Presentation of search results: the  $CL_s$  technique*, *Journal of Physics G: Nuclear and Particle Physics*, 28(10):2693, 2002